Title

Integrating Cloud Condensation Nuclei Predictions with Fast Time Resolved Aerosol Instrumentation to Determine the Hygroscopic Properties of Emissions Over Transient Drive Cycles

Authors

Vu, D.
Short, D.
Karavalakis, G.
et al.

Peer reviewed

Integrating Cloud Condensation Nuclei Predictions with Fast Time Resolved Aerosol Instrumentation to Determine the Hygroscopic Properties of Emissions Over Transient Drive Cycles

D. Vu, D. Short, G. Karavalakis, T. D. Durbin & A. Asa-Awuku

Integrating Cloud Condensation Nuclei Predictions with Fast Time Resolved Aerosol Instrumentation to Determine the Hygroscopic Properties of Emissions Over Transient Drive Cycles

D. Vu,[1,2] D. Short,[1,2] G. Karavalakis,[1,2] T. D. Durbin,[1,2] and A. Asa-Awuku[1,2]

[1]*Department of Chemical and Environmental Engineering, Bourns College of Engineering, University of California—Riverside, Riverside, California, USA*
[2]*Bourns College of Engineering, Center for Environmental Research and Technology (CE-CERT), Riverside, California, USA*

The physical and chemical properties of aerosols emitted from vehicles can vary in composition under different driving conditions. Thus, characterizing ephemeral changes in aerosol cloud condensation nuclei (CCN) activity and apparent hygroscopicity for vehicle-testing procedures conducted over transient drive cycles can be challenging. To evaluate CCN activity of these emitted aerosols, a closure method integrating traditional CCN measurements with fast time resolved aerosol instrumentation typically used to measure engine exhaust was utilized. Calibration of the method predicted activation diameters, D_d, within 10% and 15% of D_d derived from Köhler theory for two stable sources, aerosolized ammonium sulfate and α-pinene secondary organic aerosol, respectively. It was then applied to a transient source to estimate the effect of six different ethanol and iso-butanol gasoline blends on the hygroscopic properties of emissions downstream a gasoline direct injection light duty passenger vehicle over transient drive cycles. To describe the CCN activity, a single hygroscopicity parameter, kappa, was used. Results indicate low CCN activity with kappa ranging between ~0.002 and 0.06.

1. INTRODUCTION

Aerosols that activate to form cloud droplets when exposed to a supersaturated environment greater than its characteristic critical supersaturation (*SS*) are cloud condensation nuclei (CCN). This *SS* is highly dependent on curvature (Kelvin effect) and solute (Raoult effect) properties of the aerosol (Köhler 1936; Dusek et al. 2006). By acting as CCN, aerosols can modify the microphysical properties of clouds by forming droplets that either scatter solar radiation back into space or allow energy to pass through and reach the surface of the earth, thereby indirectly influencing the radiative balance of the environment (Twomey 1974). Unfortunately, these aerosol-cloud interactions and their relationship with climate are not well defined and is currently a large contributor to the uncertainty in radiative forcing estimates (Boucher et al. 2013).

Primary combustion aerosols (biomass burning, fossil fuels, and biofuels) can contribute to the CCN budget by directly increasing the particle number concentrations in the atmosphere. If they contain a fraction of soluble material at a large enough size, they may potentially be CCN active. In addition, they can serve as seeds for more soluble material to condense onto and become CCN active (Andreae and Rosenfeld 2008 and references therein). Carbonaceous combustion aerosols are estimated to account for approximately 52–64% of the global CCN budget, with a global mean aerosol indirect effect of −0.34 W m^{-2}. Aerosols derived from fossil fuels and biofuels are predicted to have the strongest cooling effect; they make up only one third of the mass from all aerosols derived from combustion fuels but account for −0.23 W m^{-2} or two thirds of the overall forcing (Spracklen et al. 2011). These carbonaceous aerosols may play an important role in the CCN budget.

Vehicle emissions are a significant source of primary carbonaceous combustion aerosols in urban atmospheres (Rose et al. 2006). Fresh vehicle emissions have been classified with low CCN activity (Tritscher et al. 2011), which may be attributed to (*i*) insoluble materials present in the aerosols, (*ii*) an externally mixed state where the condensation of soluble material is less probable, or (*iii*) small sizes where a large fraction of these aerosols are emitted in the nucleation mode directly off the tailpipe (Andreae and Rosenfeld 2008 and references therein; Karjalainen et al. 2014). Insoluble materials in fresh vehicle emissions, predominately soot, have been

Color versions or one or more of the figures in the article can be found online at www.tandfonline.com/uast.

characterized with low hygroscopic growth (Weingartner et al. 1997; Dua et al. 1999). Furthermore, freshly emitted soot is typically in an externally mixed state, so the condensation of soluble materials has not occurred and the soot maintains low hygroscopicity (Hasegawa and Ohta 2002; Rose et al. 2011). However, recent work indicates the addition of oxygenated biofuels could modify the hygroscopic properties of diesel emissions (Happonen et al. 2013) and gasoline emissions (Short et al. 2015); the latter of which exhibited potentially high CCN activity. In addition, lower elemental carbon (EC)/ organic carbon (OC) fractions have been shown to correlate with higher water soluble organic carbon (WSOC) fractions for vehicles operating with biodiesel than when operating with diesel (Cheung et al. 2009). The lower soot formation was attributed to the higher oxygen content of the biofuels, which increased oxidation and inhibited carbon chain formation. The higher oxygen content present in the higher biofuel concentration blends may lead to an increase in the WSOC to OC ratios, thereby modifying the hygroscopicty of the emissions.

One of the most widely used biofuels in the United States is ethanol, which is commonly blended at 10% ethanol and 90% gasoline (E10). However, with the Renewable Fuel Standard (RFS2) requiring 36 billion gallons of renewable fuel to be blended into transportation fuel by 2022 (USEPA 2007) there is now interest in blending higher concentrations of ethanol into gasoline. Another biofuel, iso-butanol, is also gaining popularity due to its favorable properties when compared to gasoline. Compared to ethanol, iso-butanol is less corrosive, has a higher energy content, lower volatility, and higher tolerance to water contamination (Morela et al. 2012). The aerosol composition, size, and mixing state, which can impact the hygroscopicity of the aerosols, is dependent of the vehicle technology, fuel source, and driving conditions. With biofuel use expected to grow, it is important to understand the effect of biofuels and increasing oxygenated fuel content on the hygroscopic properties of vehicle emissions. However, research related to the hygroscopicity of emissions derived from the use of different ethanol and iso-butanol blends is limited, especially when utilized in vehicles with modern engine technologies (Short et al. 2015).

For emissions sources, composition is highly dependent on the combustion conditions, which means CCN activation can vary substantially with time (Yao et al. 2006). Number concentrations can change on a second-by-second basis (e.g., but not limited to, particle number concentration time traces available in Karavalakis et al. 2014). Consequently, scanning mobility CCN analysis (SMCA) (Moore et al. 2010) requires scan times to measure relevant particle distributions that may be too long to capture the changes on a second-by-second basis. Scanning electrical mobility measurements have scan times longer than the time in which an instantaneous vehicle acceleration occurs to obtain a full size distribution, and are not ideal for transient testing. To bypass this limitation, CCN predictions using traditional CCN measurements can be integrated with fast (~1 Hz) time resolved aerosol sizing instrumentation on a second-by-second basis. With improved scanning speeds, size distributions can be measured at much higher frequencies and used for closure studies (Asa-Awuku et al. 2011). To estimate the CCN potential of aerosols derived from a transient emission source, a method to capture the changing hygroscopicity of emissions from vehicles operating on transient drive cycles is implemented using an engine exhaust particle sizer (EEPS).

An EEPS is commonly used for measuring emissions from both transient and steady state driving cycles and roadside measurements (Ayala and Herner 2005; Wang et al. 2006; Yao et al. 2006; Karavalakis et al. 2015). Although the EEPS has a lower size resolution than the SMPS, it provides a full particle size distribution every second. The application of the EEPS for diesel exhaust has been demonstrated and found to agree with other sizing and particle number concentration measurement instruments (e.g., but not limited to, Johnson et al. 2004; Kittelson et al. 2006; Zervas and Dorlhène 2006). Johnson et al. (2004) measured size distributions using both a Scanning Mobility Particle Sizer (SMPS) and the EEPS for a diesel generator operating on steady state conditions. The size distributions obtained from the two instruments agreed well, with a ±20% deviation from the mean when comparing total counts with a TSI 3022 condensation particle counter (CPC). This was attributed to the higher sampling efficiency off the EEPS; as the higher sampling speed of the EEPs minimized diffusional losses (EEPS 10 L/min vs. SMPS 1.5 L/min) thereby measuring higher particle concentrations below 12 nm. Zervas and Dorlhène (2006) found that particle numbers measured by the EEPS were close to particle numbers measured by a CPC and an electrical low pressure impactor (ELPI) for a diesel vehicle operating at steady state speeds and the New European Driving Cycle (NEDC). In addition, the engine was equipped with multiple Diesel Particulate Filters (DPF) to test the effect of concentration. Upstream of the DPFs, the instruments measured particle numbers within an order of magnitude of each other. Downstream the DPFs, the EEPS reached its lower detection limit and there was less agreement. However, its particle numbers were still within 1–2 orders of magnitude of those measured by the CPC and ELPI.

This is the first study to integrate fast time resolved aerosol sizing instrumentation, commonly used for vehicle emissions with traditional CCN measurements. It provides a comprehensive evaluation of the method by applying it to three separate aerosol sources; two stable sources and one transient source. The first stable source is ammonium sulfate aerosolized by atomization. However, atomization can result in charge effects (Liu and Deshler 2003). Therefore, secondary organic aerosol (SOA) formed from α-pinene ozonolysis is selected as the second stable source. After the method is verified on the two well characterized sources, it is then applied to relevant emissions sources to determine the potential for fresh vehicular

emissions to activate as CCN from a chassis dynamometer. The vehicular emissions are generated from a spark ignition direct injection (SIDI) vehicle operating on various alcohol blends. The results of this study demonstrates the utility of the method on multiple aerosol sources and provides information in regards to how ethanol and iso-butanol blends impact the CCN activity of particulate matter (PM) emissions from a modern light-duty gasoline vehicle.

2. THEORY AND CLOSURE ANALYSIS

2.1. κ-Köhler Theory

Köhler theory combines thermodynamic and physical properties to predict the activation diameter at which aerosol will undergo spontaneous growth and activate to form a cloud droplet in the atmosphere (Köhler 1936). Critical activation diameters (D_d) determine the supersaturations required for cloud droplet activation for aerosols of known chemical composition (Seinfeld and Pandis 2006). Köhler theory can be defined as

$$lnS_c = \left(\frac{4A^3 \rho_w M_s}{27 \nu \rho_s M_w D_d^3} \right)^{1/2}, \quad \text{where } A = \frac{4\sigma_{s/a} M_w}{RT\rho_w} \quad [1]$$

where $\sigma_{s/a}$ is the surface tension, M_w is the molecular weight of water, R the universal gas constant, T is the sample temperature, ρ_w is the density of water, D_d is the dry activation diameter, and S_c is the critical saturation, ρ_s is the density of solute, and ν is the dissociation factor of solute. It is important to note that the critical saturation, S_c, is greater than 1, thus critical supersaturation is defined by $SS = S_c - 1$.

Köhler theory requires solute information that is not always readily available, especially for complex ambient aerosols of unknown composition. To model the CCN activity of these aerosols, a single hygroscopicity parameter, κ, that represents the compositional information can be integrated with Köhler theory to relate the aerosol dry diameter and supersaturation (Petters and Kreidenweis 2007). κ-Köhler theory is defined by

$$\kappa = \frac{4A^3}{27 D_d^3 ln^2 S_c} \quad [2]$$

The surface tension of the solution is assumed to be that of pure water. Aerosol with a κ between 0.5 and 1.4 are highly hygroscopic and exhibit significant CCN activity. Aerosol with hygroscopicity between 0.01 and 0.5 are slightly to very hygroscopic. Kappa values close to zero are considered nonhygroscopic but wettable.

Köhler theory was originally used to describe the CCN activity of simple inorganic salts. However, atmospheric aerosols are typically highly complex mixtures that may contain organic and inorganic components. Modifications have been made to Köhler theory to account for these complex aerosols, and are used to help constrain aerosol cloud interaction models by predicting CCN concentrations. However, solute information is not always readily available, and in these cases, simplifications and chemical assumptions are applied to predict CCN concentrations. Closure is one way of describing the CCN activity of aerosols of unknown chemical properties. By comparing measured CCN number concentrations to CCN concentrations that were predicted based on assumed compositional information, the accuracy of predictions can be evaluated. Closure is achieved if predicted concentrations agree with measured concentrations. Previous studies have implemented closure study methods to obtain CCN activity information with varying levels of success in regions influenced by urban sources (e.g., but not limited to, VanReken et al. 2003; Asa-Awuku et al. 2011; Padró et al. 2012).

2.2. Closure Analysis

Traditionally, CCN concentrations are predicted by applying known or assumed chemical composition information and number size distribution data to Köhler theory (Equation (1)) to determine D_d for various supersaturations ("classical" Köhler theory). Using measured size distributions and the assumption that all aerosols with a diameter above D_d activate, the size bins can be integrated from D_d up to the largest diameter in the size distribution to determine the predicted CCN concentration. If this predicted concentration agrees with measured CCN concentrations, closure is achieved. However, this classical method of closure, C-Closure, can be inefficient for aerosol samples of unknown compositions that are highly variable with time.

The apparent hygroscopicity can be determined on a second-by second basis without the need for compositional information by deriving critical activation diameters by forcing closure. Using the measured size distributions, D_d is determined by integrating the aerosol concentration from the largest size bin in the distribution down to a D_d until the number concentration, which is the calculated CCN concentration, agrees with the measured CCN concentration at a given SS (reverse fit closure, R-closure). This method to determine hygroscopicity has been previously used in closure studies from field and aircraft measurements (e.g., but not limited to Kammermann et al. 2010; Jurányi et al. 2011). With SS and D_d, κ is calculated (Equation (2)) to describe the apparent hygroscopicity of the aerosol sample. Although, exhaust emissions can be fractal and may effect the electrical mobility diameter measurements (Nakao et al. 2011), the particles are assumed to be spherical. Thus, the apparent hygroscopicity of ephemeral and transient aerosol samples in this study can be derived through R-Closure using number size distribution data acquired through the use of particle sizing instrumentation with higher time resolutions.

3. EXPERIMENTAL

3.1. Instrumentation

To compare a measured CCN concentration to an aerosol concentration, a CCN counter was operated in parallel with a TSI EEPS 3090. The EEPS spectrometer was used to obtain real time second-by-second (10 Hz) particle size distributions with 32 channels between 5.6 to 560 nm. The currents are measured 10 times per second and averaged to give a full size distribution every second. Particles are sampled at a flow rate of 10 L/min to minimize diffusional losses. Particles are charged with a unipolar corona charger and sized based on electrical mobility. With the high charging efficiency of the unipolar corona chargers, both sizing and concentrations are determined through the use of multiple electrometers (22 total, measuring the electrical current to determine the concentration).

CCN activity is measured with a Droplet Measurement Technologies, Inc. single growth column CCN Counter (CCNC). The CCNC utilizes a continuous-flow thermal gradient diffusion column to create a supersaturated environment where water vapor may condense onto CCN active aerosols to form droplets (Roberts and Nenes 2005; Lance et al. 2006). Aerosols that are exposed to a supersaturation greater than its critical supersaturation activate and form droplets in the column. The droplets are sized and counted with an optical particle counter at the exit of the instrument. The CCNC is operated at a sheath to aerosol flow rate of 10:1 at a total flow rate of 0.5 L/min. To determine the supersaturations in the column, the CCNC is calibrated regularly using aerosolized dry ammonium sulfate, $(NH_4)_2SO_4$, size distributions from a TSI SMPS and SMCA to determine D_d (Rose et al. 2008; Moore et al. 2010). The SMPS utilizes a long differential mobility analyzer (DMA 3081) and has a 135 second scan time. The particles are passed through a bi-polar krypton-85 charger, sized based on electrical mobility, and concentrations are counted using a butanol-based CPC. SMCA setup requires the CCNC to operate in parallel with a CPC after the DMA. This allows the simultaneous measurements of the total aerosol and CCN concentrations at a given supersaturation of the monodispersed aerosols. Operating the DMA in scanning voltage mode provides CCN active aerosol fraction information over a full size distribution. The SS in the column is held constant over the course of the 135 second scan. Theoretical SS values are derived from the measured D_d values.

4. EXPERIMENTAL SET UP

4.1. Stable Source Aerosols: Ammonium Sulfate and α-Pinene SOA

Before proceeding to a transient source, the method was applied to two stable sources, atomized ammonium sulfate (AS), $(NH_4)_2SO_4$, and α-pinene secondary organic aerosol (SOA) to test the validity of the method using both C-Closure and R-Closure. The hygroscopic properties of ammonium sulfate (AS) aerosols (Rose et al. 2008) and α-pinene ozonolysis (Engelhart et al. 2008) products have been well characterized, and thus, were selected for the verification. The CCNC is operated in parallel with an EEPS to obtain simultaneous size distributions from both instruments. The experimental setup is shown in Figure 1. The CCN closure using C-Closure and R-closure for both the $(NH_4)_2SO_4$ aerosols and the α-pinene SOA are presented in Figure 2.

AS aerosols were atomized from an aqueous salt solution of AS (Acros, 99.5%) and Millipore$^{©}$ DI water (18 mΩ, < 100 ppb), dried, and then passed over ^{210}Po to neutralize the electrostatic charge of the aerosols. To bypass possible charging errors associated with atomization, the method was further verified by oxidizing α-pinene with ozone in a dark 12.5 m³ 2mil FEP environmental chamber available at the Center for Environmental Research and Technology (CE-CERT) Atmospheric Processes Laboratory (APL). A more detailed description of the chamber is available in Nakao et al. (2011). Prior
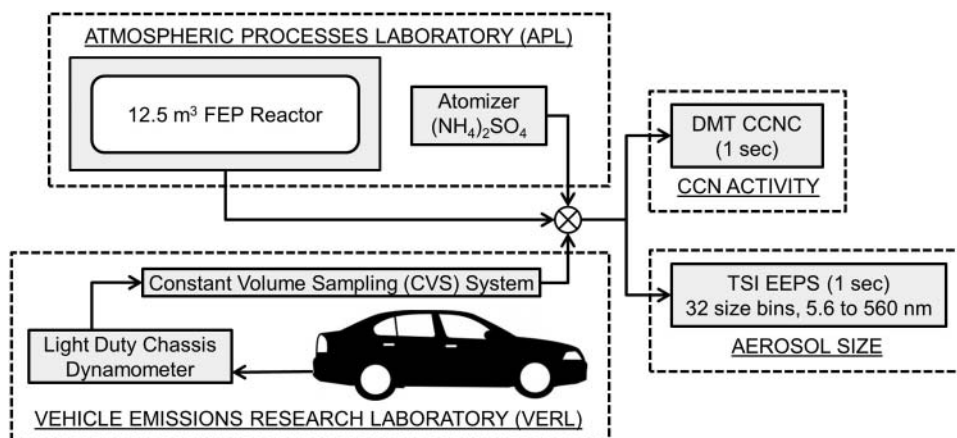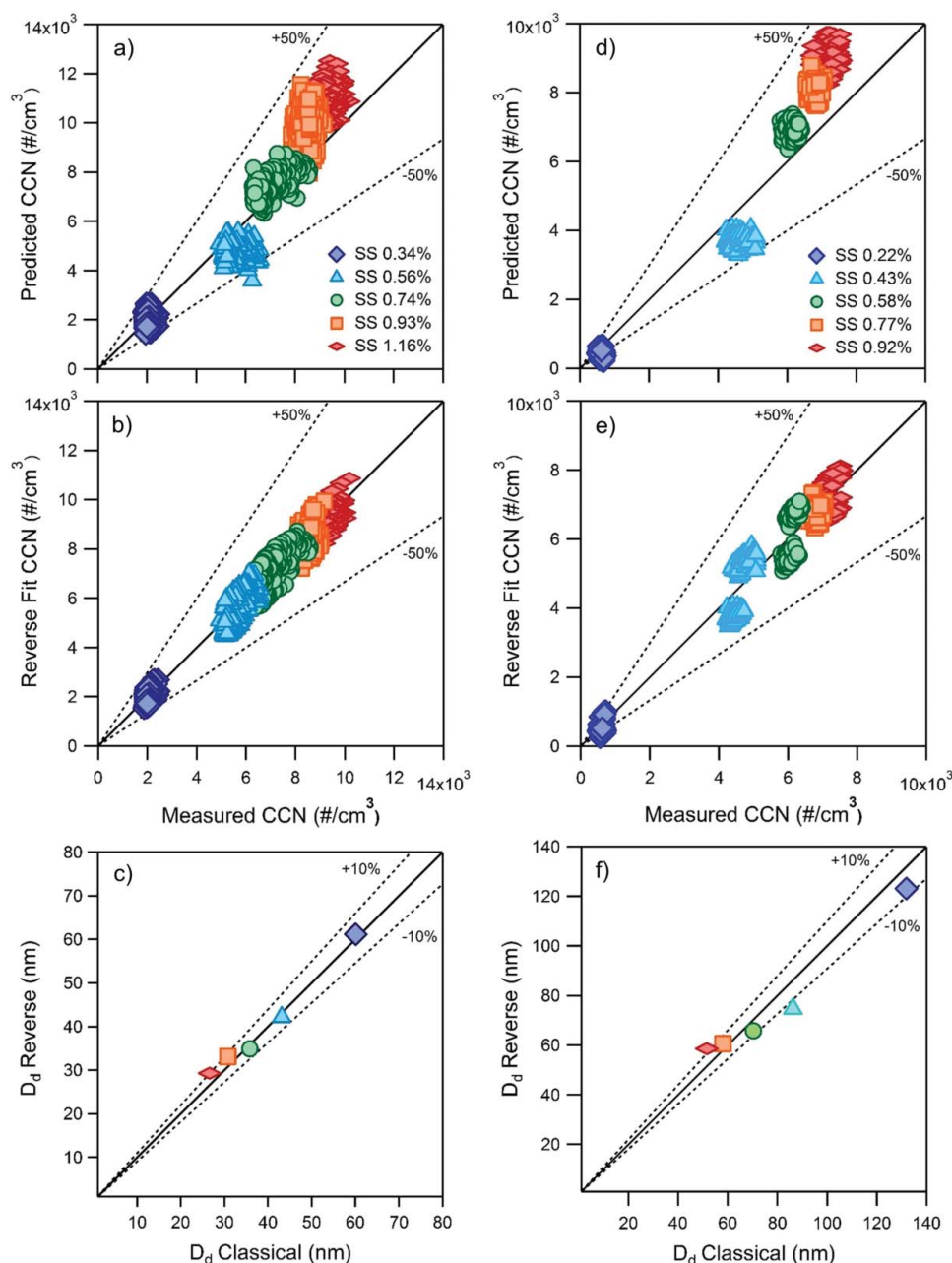

FIG. 1. Experimental Setup.

FIG. 2. Calibrations using an atomized aerosol and a complex organic aerosol. Ammonium sulfate (a) C-Closure, (b) R-Closure, (c) predicted D_d from R-Closure vs. predicted D_d from C-Closure; α-pinene SOA, (D) C-Closure, (E) R-Closure, and (f) predicted D_d from R-Closure vs. predicted D_d from C-Closure.

to each experiment, the reactor was cleaned with pure air (Aadco 737 series air purification system). Ozone was generated by passing clean air over a Pen-Ray ultraviolet lamp (Part No. B131799, Ultra-Violet Products Inc.) and monitored with a Teledyne 400E ozone monitor. After the ozone concentrations stabilized, the α-pinene (Sigma Aldrich, 98%) was injected by passing clean air over the compound in a glass injection manifold. All experiments were completed using approximately 25 ppb of α-pinene. Any slight changes in initial concentrations <40 ppb have been shown to not effect the

CCN activity of the SOA (Engelhart et al. 2008). The effective density used for α-pinene SOA predictions was 1.3 g/cm^3 (Alfarra et al. 2006), and the molecular weight was 180 g/mol (Engelhart et al. 2008). Complete solubility was assumed with no dissociation ($\nu = 1$).

4.2. Test Fuels

A total of six ethanol and iso-butanol biofuels were selected for the fuel blends. The ethanol blends include E10 (10%

ethanol and 90% gasoline), E15, E20. E10 was selected as the baseline fuel. The iso-butanol blends include B16, B24, and B32 and were selected as the oxygen equivalent of E10, E15, and E20, respectively. All fuels were match-blended according to Reid vapor pressure, and oxygen content to maintain the fuel properties of the gasoline. A more detailed description regarding fuel and blending properties are available in Karavalakis et al. 2014.

4.3.   Emissions Testing and Test Cycles

Measurements were conducted in the University of California, Riverside (UCR) CE-CERT Vehicle Emissions Research Laboratory (VERL). VERL is equipped with a Burke E. Porter 48-inch single roller chassis dynamometer, and a constant volume sampler (CVS) for certification quality measurements. The instruments sampled directly off of the CVS tunnel. The experimental setup is shown in Figure 1.

A 2012 Mercedes Benz E350 (MBE350) with a spray-guided SIDI (SG-SIDI) engine was tested over the Federal Test Procedure (FTP) and California Unified Cycle (UC). The FTP is representative of city driving conditions for light duty vehicles and consists of three phases: cold start/cold three-way catalyst (TWC) converter (Phase 1), transient/stabilize (Phase 2), and hot start/warm TWC converter (Phase 3). Phase 2 is the stabilized phase. The car is turned off during the hot soak (between phases 2 and 3). The driving pattern in Phase 3 is identical to Phase 1 with the exception that the TWC is now warm. The UC is similar to the FTP, but has higher average speeds with a higher maximum speed, less idling periods, and a greater maximum rate of acceleration. Additional information in regards to the test procedures and driving cycles are available in Karavalakis et al. (2013) and the online supplementalary information.

5.   RESULTS

5.1.   Ammonium Sulfate and α-Pinene SOA: Closure Assessment

C-closure and R-closure for AS aerosols is shown in Figures 2a and b. Figure 2a shows a slight over prediction when using C-closure for the higher supersaturations of 0.93% and 1.16%; this can be attributed to vapor depletion effects. The higher aerosol number leads to water vapor depletion in the CCN counter column, thus CCN active aerosols that would normally activate do not have enough water available to grow to a detectable size (Lathem and Nenes 2003). However, when applying R-closure, the calculated concentrations are lower (Figure 2b), which minimizes the effects seen by water depletion for this reverse fit method. C-closure and R-closure for α-pinene SOA is shown in Figures 2d–e. Similar to $(NH_4)_2SO_4$ aerosols, over prediction is observed for the α-pinene SOA C-Closure.

The critical diameter (in Figures 2c and f) is predicted and derived from the forced closure data set in Figures 2b and 2e. The critical diameters are compared to literature values (Köhler Theory) used in Figures 2a and d. The D_d derived from both closure methods for AS and α-pinene secondary organic aerosols fell within 10% and 15%, respectively. This slight deviation for the α-pinene SOA may be due to the presence of organics which have been shown to make CCN closure more difficult to achieve (e.g., but not limited to Cantrell et al. 2001; Medina et al. 2007; Martin et al. 2011). There is strong agreement between D_d derived from C-closure and R-closure for both the AS and α-pinene SOA which shows that size distributions measured by an EEPS can be used to predict CCN concentrations using R-closure.

5.2.   Selecting an Appropriate *SS*

A 2012 Kia Optima with a SIDI engine, operating on E20 was the first vehicle available for the study. Thus, preliminary data collected from this vehicle and fuel determined an appropriate *SS* to best achieve closure. R-closure was applied to three separate FTP cycles, where the CCNC was operated at a constant *SS* for the duration of each cycle (0.19%, 0.58%, and 0.85%). The range of *SS* were selected to represent the different supersaturations characterized for the different cloud types in the atmosphere (Seinfeld and Pandis 2006).

For the two lowest supersaturations, FTP1 (*SS* 0.18%) and FTP2 (*SS* 0.58%), the measured CCN concentrations do not change significantly; the CCN concentrations are $<<100$ #/cm^{-3} with a large fraction of the values below 50 #/cm^{-3} throughout the cycle (Figures 3a–c). In addition, there is greater variability in predicted CCN concentrations for these lower supersaturations. This lack of closure and variability may be due to a) the lower SS, where the small temperature gradient is difficult to maintain, fluctuations in the instrument SS can result, and the signal to noise ratio may increase, thereby resulting in poorer CCN measurements (Roberts and Nenes 2005); and b) the large vertical spread, which results from the calculated CCN from R-Closure from the EEPS data set. With low SS, and thus, low CCN concentrations, only the most hygroscopic of the sample aerosol (the upper end of the size distribution) are captured. The EEPS approximates a log-normal fit (Johnson et al. 2004; Xue et al. 2015); the CCN concentrations are derived from few size bins, resulting in fewer approximated counts. Previous work has shown the EEPS reporting lower particle concentrations than those reported by the SMPS in the high accumulation mode range due to more fractal like particles (Zimmerman et al. 2014; Xue et al. 2015).

Significant differences were not observed between the phases as the D_d were consistently high (Figure 3d). The lower *SS* only captures the most hygroscopic aerosols and is not a good reflection of the changing CCN activity. For the high *SS*, FTP3 (SS 0.85%), instrument counting statistics improved
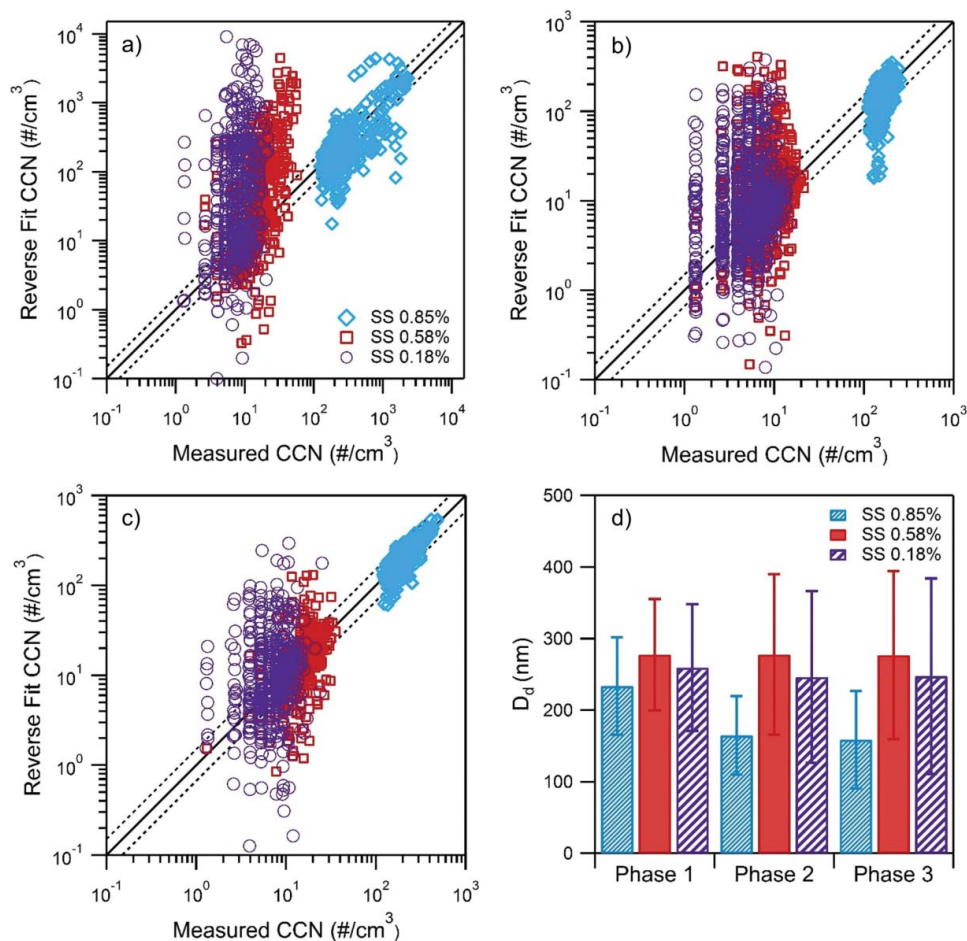
FIG. 3. CCN R-Closure (a) Phase 1, (b) Phase 2, (c) Phase 3. Solid lines 1:1 line, dashed is ±10%. (s) Averaged D_d for each phase of driving cycle.

with the higher CCN concentrations and the strongest closure was achieved. With higher CCN concentrations, a stronger signal was obtained, which allowed for stronger closure. Phase 2 (Figure 3b) and Phase 3 (Figure 3c) produce more hygroscopic particles than those emitted in Phase 1 (Figure 3a). Data are shown from the highest measured SS for the duration of the emissions testing because the high SS had the strongest closure and allowed differences in D_d to be observed (Figure 3d).

5.3. Iso-Butanol and Ethanol Gasoline Blends for a Gasoline Direct Injection Vehicle

The effect of ethanol and iso-butanol gasoline blends on the CCN activity of fresh emissions was investigated. CCN concentrations and size distribution measurements were collected for the MBE350 using the six different ethanol and iso-butanol blends described in Section 4.2. The CCNC was operated at SS between 0.83% and 1.16% over the course of the transient aerosol tests. R-Closure (Figure 4) was applied to estimate D_d.

Overall, the apparent hygroscopicity is consistently low for both biofuels. Iso-butanol blends were observed to produce

aerosols that were slightly more hygroscopic than that produced by the ethanol blends. Single hygroscopicity parameter, κ, values ranged from 0.0021 to 0.062 for iso-butanol blends and 0.0019 to 0.022 for ethanol blends (Figure 5). The error bars are the average standard deviation derived from the repetition of experiments. The errors associated with the final kappa values, when available, are small and indicate repeatability between measurements. Although this is not a significant difference between the different ethanol and iso-butanol blends, it is consistent with results from Short et al. (2015), who observed lower water insoluble mass fractions for the iso-butanol blends. The effect of alcohol concentrations was also observed; the lower alcohol blends exhibited higher κ values. Karavalakis et al. (2015) reported lower number concentrations of accumulation mode particles for E20 and B32 and in some cases, smaller geometric mean diameters were observed as well when they tested a SG-SIDI vehicle over the FTP and UC cycles. The low hygroscopicity may also be attributed to non-hygroscopic composition such as soot found in the smaller size range. Karavalakis et al. (2015) reported high soot emissions for B24 relative to other iso-butanol blends which is consistent with the low κ value for this fuel. In addition, E15 had
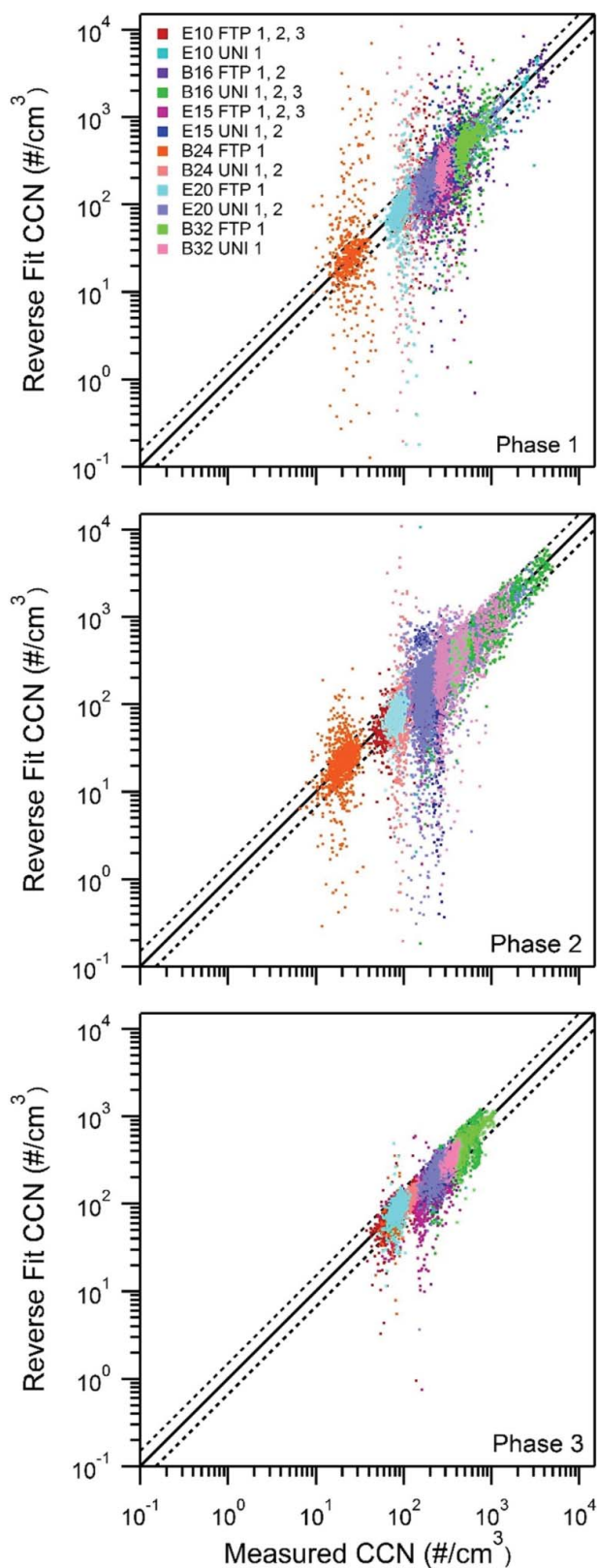
FIG. 4. Effects of Phases 1, 2, and 3 on closure.

low soot emissions relative to the other ethanol blends which is consistent with the high κ values for this fuel. This is consistent with fresh emissions not being very hygroscopic, which may require very large diameters or water soluble compounds for the CCN to activate.

Effects among the cycles were observed for the driving patterns; κ ranged from 0.0021 to 0.017 for the FTP and 0.0019 to 0.062 for the UC cycle. More hygroscopic particles were observed for the UC cycle, which exhibits higher speeds. The higher hygroscopicity agrees with Short et al. (2015), who observed greater κ values for high steady state speeds than that of lower steady state speeds for a SIDI vehicle operating on ethanol and iso-butanol blends. In addition, the cold-start influence was particularly strong, where for most fuels the cold-start phase emitted the least hygroscopic particles with kappa ranging from 0.0021 to 0.014. Soot emissions are highest during phase 1 operating on the same biofuel blends as a result of the TWC being below its light-off temperature and thus, resulting in lower catalytic efficiency (Karavalakis et al. 2015). Phase 2 and 3 produced more hygroscopic materials and kappa values ranged from 0.0019 to 0.027 and 0.0048 to 0.062, respectively. Closure improves with the more hygroscopic aerosols in Phase 3 (Figures 4 and 5). Improvements in closure can also be attributed to the calculated concentrations staying above the lower detection limit of the EEPs.

6. SUMMARY

This is the first closure study to combine fast resolution CCN activation information from both a continuous CCN counter and an EEPS to study CCN activity for fresh vehicle emissions operating on ethanol and iso-butanol blends. The instrumentation and analytical methods presented are able to characterize the rapidly changing particle composition generated by vehicle accelerations. Six ethanol and iso-butanol blends were tested on a single light-duty SIDI vehicle driving on UC and FTP cycles. The fuels were selected at random for vehicle testing and initial CCN evaluation began with E20 fuel. The greatest hygroscopicity differences in fresh emissions were observed at higher supersaturations. The results suggest that the method is aptly used at higher supersaturations. At higher *SS*, small changes in aerosol composition affect droplet activation changes and derived critical diameters are more readily discerned. Although the EEPS may lack time resolution in size information, the rapid changes in hygroscopicity of the transient aerosol system with this system can be observed. With the use of fast-time resolved CCN analysis, such as the method presented here, sources with rapidly changing aerosol composition (e.g., combustion studies, aircraft-based atmospheric measurements) can be observed.

The shifts in kappa reflect the sensitivity of aerosol composition to the transient nature of the cycles and different fuels. The least hygroscopic particles occurred during Phase 1 when the catalyst was below its light-off temperature and the engine
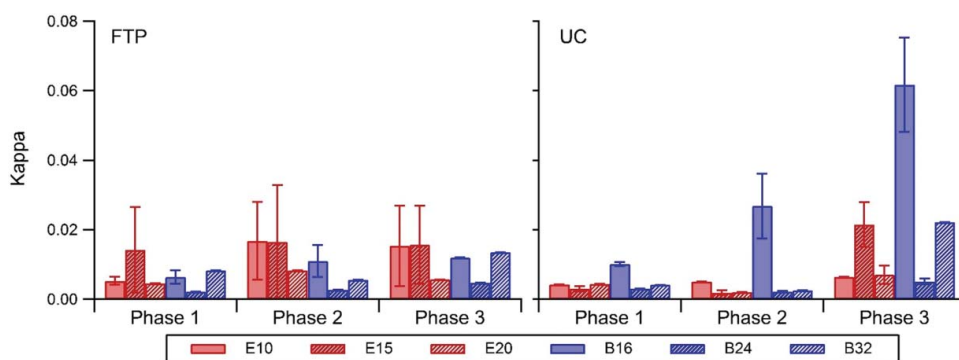
FIG. 5. Effects of iso-butanol and ethanol fuel blends. Kappa values presented for each phase for supersaturations between 0.83% and 1.16%.

was cold. These results are consistent with the production of soot, from inefficient combustion. The most hygroscopic particles occurred during phases 2 and 3 after the catalyst was warm. Thus particles emitted during warm-start driving conditions will most likely uptake water. The composition of emissions, particularly aerosol, can significantly change during transient drive cycles. Driving patterns inevitably change, and thus the extent to which each vehicle spends in each phase will modify particle hygroscopicity.

Overall, these fresh emissions exhibit relatively low kappa values ($\kappa < 0.1$). Fresh vehicle emissions initially have hydrophobic properties, which will inhibit the uptake of water and limit the ability to activate as cloud droplets. As a result, localized aerosols near urban sources can exhibit high variability in CCN activity. However, at regional scales where the aerosols have undergone atmospheric aging, the hygroscopicity can be modified under atmospheric conditions, such as oxidation and the condensation of soluble materials (Wittbom et al. 2014) and can exhibit higher CCN activity (Asa-Awuku et al. 2011). Small amounts of soluble material can have large effects on the water uptake properties of insoluble compounds (Bilde and Svenningsson 2004). This information collectively suggests that the aging of vehicle emission aerosols could exhibit different physical and chemical properties than the fresh aerosols emitted in this study.

To be able to account for atmospheric interactions such as transport, coagulation, and transformations, modeling atmospheric interactions is highly dependent on source emissions data. Fresh emissions may not directly play a large role in regional indirect effects. However, aerosol emissions from vehicles may be subject to rapid physical and chemical changes. With vehicle technologies changing and new fuel formulations penetrating the market, the impact of aerosol hygroscopicity for regional visibility and cloud droplet formation must be assessed. Information in regards to the amount and how CCN active these primary emissions are important as it provides a measure of their direct contribution into the atmosphere and can aid in predicting its atmospheric aging behavior in the presence of other aerosol or gas phase species. Additional work is required to understand the evolution of

fresh emissions downwind from the initial source; the processed aerosols are more likely to impact regional visibility and modify clouds. The modification of hygroscopic properties due to atmospheric aging must be explored next and compared to the results presented here.

ACKNOWLEDGMENTS

FUNDING

SUPPLEMENTAL MATERIALS

Supplemental data for this article can be accessed on the publisher's website.

REFERENCES

Alfarra, M. R., Paulsen, D., Gysel, M., Garforth, A. A., Dommen, J., Prévôt, A. S. H., Worsnop, D. R., Baltensperger, U., and Coe, H. (2006). A Mass Spectrometric Study of Secondary Organic Aerosols Formed from the Photooxidation of Anthropogenic and Biogenic Precursors in a Reaction Chamber. *Atmos. Chem. Phys.*, 6:5279–5293.

Andreae, M. O., and Rosenfeld, D. (2008). Aerosol–Cloud–Precipitation Interactions. Part 1. The Nature and Sources of Cloud-Active Aerosols. *Earth Sci. Rev.*, 89:13–41, doi:10.1016/j.earscirev.2008.03.001.

Asa-Awuku, A., R.H. Moore, R.H., Nenes, A., Bahreini, R., Holloway, J. S., Brock, C.A., Middlebrook, A. M., Ryerson, T. B., Jimenez, J. L., DeCarlo,

P. F., Hacobian, A., Weber, R. J., Stickel, R., Tanner, D. J., and Huey, L. G. (2011). Airborne Cloud Condensation Nuclei Measurements During the 2006 Texas Air Quality Study. *J. Geophys. Res.*, 116:D11201, doi:10.1029/2010JD014874.

Ayala, A., and Herner, J. (2005). Transient Ultrafine Particle Emission Measurements with a New Fast Particle Aerosol Sizer for a Trap Equipped Diesel Truck. SAE Technical Paper 2005-01-3800, doi:10.4271/2005-01-3800.

Bilde, M., and Svenningsson, B. (2004). CCN Activation of Slightly Soluble Organics: The Importance of Small Amounts of Inorganic Salt and Particle Phase. *Tellus. B,*. 56:128–134, doi:10.1111/j.1600-0889.2004.00090.

Boucher, O., Randall, D., Artaxo, P., Bretherton, C., Feingold, G., Forster, P., Kerminen, V.-M., Kondo, Y., Liao, H., Lohmann, U., Rasch, P., Satheesh, S. K., Sherwood, S., Stevens, B., and Zhang, X. Y. (2013). Clouds and Aerosols. In: *Climate Change 2013: The Physical Science Basis. Contribution of Working Group I to the Fifth Assessment Report of the Intergovernmental Panel on Climate Change*, T. F. Stocker, D. Qin, G.-K. Plattner, M. Tignor, S. K. Allen, J. Boschung, A. Nauels, Y. Xia, V. Bex and P. M. Midgley, eds. Cambridge University Press, Cambridge, UK, pp. 571–658.

Cantrell, W., Shaw, G., Cass, G., Chowdhury, Z., Hughes, L. S., Prather, K., Guazzotti, S., and Coffee, K. R. (2001). Closure Between Aerosol Particles and Cloud Condensation Nuclei at Kaashidhoo Climate Observatory. *J. Geophys. Res.*, 106:D22.

Cheung, K. L., Polidori, A., Ntziachristos, L., Tzamkiozis, T., Samaras, Z., Cassee, F. R., Gerlofs, M., and Sioutas, C. (2009). Chemical Characteristics and Oxidative Potential of Particulate Matter Emissions from Gasoline, Diesel, and Biodiesel Cars. *Env. Sci. Tech.*, 43:6334–6340.

Dua, S., Hopke, P., and Raunemaa, T. (2009). Hygroscopicity of Diesel Aerosols. *Water Air Soil Pollut.*, 112:247–257.

Dusek, U., Frank, G. P., Hildebrandt, L., Curtius, J., Schneider, J., Walter, S., Chand, D., Drewnick, F., Hings, S., Jung, D., Borrmann, S., and Andreae, M. O. (2006). Size Matters More Than Chemistry for Cloud-Nucleating Ability of Aerosol Particles. *Science*, 312:1375–1378.

Engelhart, G. J., Asa-Awuku, A., Nenes, A., and Pandis, S. N. (2008). CCN Activity and Droplet Growth Kinetics of Fresh and Aged Monoterpene Secondary Organic Aerosol. *Atmos. Chem. Phys.*, 8:3937–3949, doi:10.5194/acp-8-3937-2008.

Happonen, M., Heikkilä, J., Aakko-Saksa, P., Murtonen, T., Lehto, K., Rostedt, A., Sarjovaara, T., Larmi, M., Keskinen, J., and Virtanen, A. (2013). Diesel Exhaust Emissions and Particle Hygroscopicity with HVO Fuel-Oxygenate Blend. *Fuel*, 103:380–386, doi:10.1016/j.fuel.2012.09.006.

Hasegawa, S., and Ohta, S. (2002). Some Measurements of the Mixing State of Soot-Containing Particles at Urban and Non-Urban Sites. *Atmos. Environ.* 36:3899–3908.

Johnson, T., Caldow, R., Pöcher, A., Mirme, A., and Kittelson, D. (2004). A New Electrical Mobility Particle Sizer Spectrometer for Engine Exhaust Particle Measurements. SAE Technical Paper 2004-01-1341, doi:10.4271/2004-01-1341.

Jurányi, Z., Gysel, M., Weingartner, E., Bukowiecki, N., Kammermann, L., and Baltensperger, U. (2011). A 17 Month Climatology of the Cloud Condensation Nuclei Number Concentration at the High Alpine Site Jungfraujoch. *J. Geophys. Res.*, 116:D10.

Kammermann, L., Gysel, M., Weingartner, E., Herich, H., Cziczo, D. J., Holst, T., Svenningsson, B., Arneth, A., and Baltensperger, U. (2010). Subarctic Atmospheric Aerosol Composition: 3. Measured and Modeled Properties of Cloud Condensation Nuclei. *J. Geophys. Res.*, 115:D04202, doi:10.1029/2009JD012447.

Karavalakis, G., Short, D., Vu, D., Villela, M., Asa-Awuku, A., and Durbin, T. (2013). Criteria Emissions, Particle Number Emissions, Size Distributions, and Black Carbon Measurements from PFI Gasoline Vehicles Fuelled with Different Ethanol and Butanol Blends. SAE Technical Paper 2013-01-1147.

Karavalakis, G., Short, D., Vu, D., Villela, M., Asa-Awuku, A., and Durbin, T. (2014). Evaluating the Regulated Emissions, Air Toxics, Ultrafine Particles, and Black Carbon from SI-PFI and SI-DI Vehicles Operating on Different Ethanol and Iso-Butanol Blends. *Fuel*, 128:410–21.

Karavalakis, G., Short, D., Vu, D., Russell, R., Asa-Awuku, A., Jung, H., Johnson, K., and Durbin, T. (2015). The Impact of Ethanol and Iso-Butanol Blends on Gaseous and Particulate Emissions from Two Passenger Cars Equipped with Spray-Guided and Wall-Guided Direct Injection SI (spark ignition) Engines. *Energy*, 82:168–179, doi:10.1016/j.energy.2015.01.023.

Karjalainen, P., Pirjola, L., Heikkilä, J., Lähde, T., Tzamkiozis, T., Ntziachristos, L., Keskinen, J., and Rönkkö, T. (2014). Exhaust Particles of Modern Gasoline Vehicles: A Laboratory and an On-Road Study. *Atmos. Envir.*, 97:262–270, ISSN 1352-2310, doi:10.1016/j.atmosenv.2014.08.025.

Kittelson, D.B., Watts, W.F., Johnson, J.P., Rowntree, C., Payne, M., Goodier, S., Warrens, C., Preston, H., Zink, U., Ortiz, M., Goersmann, C., Twigg, M.V., Walker, A.P., and Caldow, R. (2006). On-Road Evaluation of Two Diesel Exhaust After Treatment Devices. *J. Aerosol Sci.*, 37:1140–1151.

Köhler, H. (1936). The Nucleus in and the Growth of Hygroscopic Droplets. *Trans. Farad. Soc.*, 32:1152–1161.

Lance, S., Medina, J., Smith, J. N., and Nenes, A. (2006). Mapping the Operation of the DMT Continuous Flow CCN Counter. *Aeros. Sci. Tech.*, 40:242–254.

Lathem, T. L., and Nenes, A. (2003). Water Vapor Depletion in the DMT Continuous-Flow CCN Chamber: Effects on Supersaturation and Droplet Growth. *Aer. Sci. Tech.*, 45:916–923.

Liu, P., and Deshler, T. (2003). Causes of Concentration Differences Between a Scanning Mobility Particle Sizer and a Condensation Particle Counter. *Aer. Sci. Tech.*, 37:604–615.

Martin, M., Chang, R. Y.-W., Sierau, B., Sjogren, S., Swietlicki, E., Abbatt, J. P. D., Leck, C., and Lohmann, U. (2011). Cloud Condensation Nuclei Closure Study on Summer Arctic Aerosol. *Atmos. Chem. Phys.*, 11:11335–11350, doi:10.5194/acp-11-11335-2011.

Medina, J., Nenes, A., Sotiropoulou, R.-E. P., Cottrell, L. D., Ziemba, L. D., Beckman, P. J., and Griffin, R. J. (2007). Cloud Condensation Nuclei Closure During the International Consortium for Atmospheric Research on Transport and Transformation 2004 Campaign: Effects of Size-Resolved Composition. *J. Geophys. Res.*, 112:D10S31, doi:10.1029/2006JD007588.

Moore, R. H., Nenes, A., and Medina, J. (2010). Scanning Mobility CCN Analysis—A Method for Fast Measurements of Size-Resolved CCN Distributions and Activation Kinetics. *Aer. Sci. Tech.*, 44:861–871.

Morela, S.S., Tornatore, C., Marchitto, L., Valentino, G., and Corcione, F.E. (2012). Experimental Investigation of Butanol-Gasoline Blends Effects on the Combustion Process in a SI Engine. *Intl. J. Energy Env. Eng.*, 3:6.

Nakao, S., Shrivastava, M., Nguyen, A., Jung, H. and Cocker, III, D. (2011). Interpretation of Secondary Organic Aerosol Formation from Diesel Exhaust Photo-oxidation in an Environmental Chamber. *Aer. Sci. Tech.*, 45:954–962.

Padró, L. T., Moore, R. H., Zhang, X., Rastogi, N., Weber, R. J., and Nenes, A. (2012). Mixing State and Compositional Effects on CCN Activity and Droplet Growth Kinetics of Size-Resolved CCN in an Urban Environment. *Atmos. Chem. Phys.*, 12:10239–10255.

Petters, M. D. and Kreidenweis, S. M. (2007). A Single Parameter Representation of Hygroscopic Growth and Cloud Condensation Nucleus Activity. *Atmos. Chem. Phys.*, 7:1961–1971, doi:10.5194/acp-7-1961-2007.

Roberts, G. C., and Nenes, A. (2005). A Continuous-Flow Streamwise Thermal-Gradient CCN Chamber for Atmospheric Measurements. *Aer. Sci. Tech.*, 39:206–221, doi: 10.1080/027868290913988.

Rose, D., Wehner, B., Ketzel, M., Engler, C., Voigtländer, J., Tuch, T., and Wiedensohler, A. (2006). Atmospheric Number Size Distributions of Soot Particles and Estimation of Emission Factors. *Atmos. Chem. Phys.*, 6:1021–1031, doi:10.5194/acp-6-1021-2006.

Rose, D., Gunthe, S. S., Mikhailov, E., Frank, G. P., Dusek, U., Andreae, M. O., and Pöschl, U. (2008). Calibration and Measurement Uncertainties of a Continuous-Flow Cloud Condensation Nuclei Counter (DMT-CCNC): CCN Activation of Ammonium Sulfate and Sodium Chloride Aerosol

Particles in Theory and Experiment. *Atmos. Chem. Phys.*, 8:1153–1179, doi:10.5194/acp-8-1153-2008.

Rose, D., Gunthe, S. S., Su, H., Garland, R. M., Yang, H., Berghof, M., Cheng, Y. F., Wehner, B., Achtert, P., Nowak, A., Wiedensohler, A., Takegawa, N., Kondo, Y., Hu, M., Zhang, Y., Andreae, M. O., and Pöschl, U. (2011). Cloud Condensation Nuclei in Polluted Air and Biomass Burning Smoke Near the Mega-City Guangzhou, China – Part 2: Size-Resolved Aerosol Chemical Composition, Diurnal Cycles, and Externally Mixed Weakly CCN-Active Soot Particles. *Atmos. Chem. Phys.*, 11:2817–2836, doi:10.5194/acp-11-2817-2011.

Seinfeld, J. H., and Pandis, S. N. (2008). *Atmospheric Chemistry and Physics: From Air Pollution to Climate Change*, 2nd Edition. John Wiley & Sons, New York.

Short, D., Vu, D., Durbin, T., Karavalakis, G., and Asa-Awuku, A. (2015). Particle Speciation of Iso-Butanol and Ethanol Blended Gasoline in Light-Duty Port Fuel Injection, Vehicles. *J. Aerosol Sci.*, 84:39–52.

Spracklen, D. V., Carslaw, K. S., Pöschl, U., Rap, A., and Forster, P. M. (2011). Global Cloud Condensation Nuclei Influenced by Carbonaceous Combustion Aerosol. *Atmos. Chem. Phys.*, 11:9067–9087, doi:10.5194/acp-11-9067-2011.

Tritscher, T., Juranyi, Z., Martin, M., Chirico, R., Gysel, M., Heringa, M. F., DeCarlo, P.F., Sierau, B., Prevot, A.S.H., Weingartner, E., and Baltenspreger, U. (2011). Changes of Hygroscopicity and Morphology During Ageing of Diesel Soot. *Environ. Res. Lett.*, 6, 034026. doi:10.1088/1748-9326/6/3/034026.

Twomey, S. (1974). Pollution and the Planetary Albedo. *Atmos. Environ.*, 8:1251–1256.

U.S. Environmental Protection Agency. (2009). Fuels and Fuel Additives, Renewable Fuel Standard (RFS2), Available at <http://www.epa.gov/otaq/fuels/renewablefuels/regulations.htm>.

VanReken, T. M., Rissman, T. A., Roberts, G. C., Varutbangkul, V., Jonsson, H. H., Flagan, R. C., and Seinfeld, J. H. (2003). Toward Aerosol/Cloud Condensation Nuclei (CCN) Closure During CRYSTAL-FACE. *J. Geophys. Res.*, 108:D20, doi:10.1029/2003JD003582.

Wang, J., Storey, J., Domingo, N., Huff, S., Thomas, J., and West, B. (2006). Studies of Diesel Engine Particle Emissions During Transient Operations Using an Engine Exhaust Particle Sizer. *Aer. Sci. and Tech.*, 40:1002–1015.

Weingartner, E., Burtscher, H., and Baltensperger, U. (1997). Hygroscopic Properties of Carbon and Diesel Soot Particles. *Atmos. Environ.*, 31:2311–2327.

Wittbom, C., Eriksson, A. C., Rissler, J., Carlsson, J. E., Roldin, P., Nordin, E. Z., Nilsson, P. T., Swietlicki, E., Pagels, J. H., and Svenningsson, B. (2014). Cloud Droplet Activity Changes of Soot Aerosol Upon Smog Chamber Ageing. *Atmos. Chem. Phys.*, 14:9831–9854, doi:10.5194/acp-14-9831-2014.

Xue, J., Li, Y., Wang, X., Durbin, T., Johnson, K.C., Karavalakis, G., Asa-Awuku, A., Villela, M., Quiros, D., Hu, S., Huai, T., Ayala, A., and Jung, H. (2015). Comparison of Vehicle Exhaust Particle Size Distributions by SMPS and EEPS During Steady State Operating Conditions. *Aer. Sci. Tech.*, 9(10):984–996.

Yao, X. H., Lau, N. T., Fang, M., and Chan, C. K. (2006). On the Time-Averaging of Ultrafine Particle Number Size Spectra in vehicular Plumes. *Atmos. Chem. Phys.*, 6:4801–4807, doi:10.5194/acp-6-4801-2006.

Zervas, E., and Dorlhène, P. (2006). Comparison of Exhaust Particle Number Measured by EEPS, CPC, and ELPI. *Aer. Sci. Tech.*, 40:977–984.

Zimmerman, N., Pollitt, K. J. G., Jeong, C. H., Wang, J. M., Jung, T., Cooper, J. M., Wallace, J. S., and Evans, G. J. (2014). Comparison of Three Nanoparticle Sizing Instruments: The Influence of Particle Morphology. *Atmos. Environ.*, 86:140–14.